THE JOURNAL OF PHYSICAL CHEMISTRY C
A JOURNAL OF THE AMERICAN CHEMICAL SOCIETY

pubs.acs.org/JPCC
Perspective

Lessons Learned from Catalysis to Qubits: General Strategies to Build Accessible and Accurate First-Principles Models of Point Defects

Gil M. Repa and Lisa A. Fredin*

Cite This: *J. Phys. Chem. C* 2023, 127, 21930−21939
Read Online
ACCESS | Metrics & More | Article Recommendations

ABSTRACT: Defects and dopants play critical roles in defining the properties of a material. Achieving a mechanistic understanding of how such properties arise is challenging with current experimental methods, and computational approaches suffer from significant modeling limitations that frequently require *a posteriori* fitting. Consequently, the pace of dopant discovery as a means of tuning material properties for a particular application has been slow. However, recent advances in computation have enabled researchers to move away from semiempirical schemes to reposition density functional theory as a predictive tool and improve the accessibility of highly accurate first-principles methods to all researchers. This Perspective discusses some of these recent achievements that provide more accurate first-principles geometric, thermodynamic, optical, and electronic properties simultaneously. Advancements related to supercells, basis sets, functionals, and optimization protocols, as well as suggestions for evaluating the quality of a computational model through comparison to experimental data, are discussed. Moreover, recent computational results in the fields of energy materials, heterogeneous catalysis, and quantum informatics are reviewed along with an evaluation of current frontiers and opportunities in the field of computational materials chemistry.

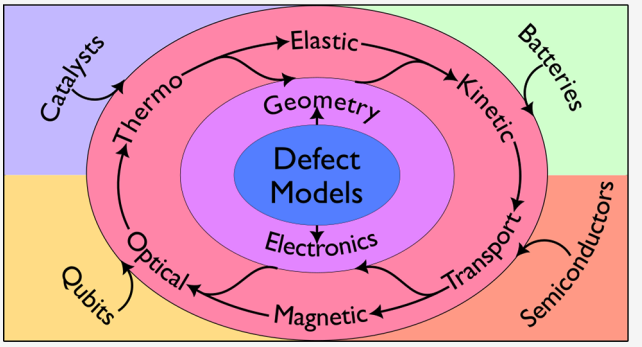

INTRODUCTION

Altering material properties through defects and dopants has long been a means of conferring new functionality to known materials. Indeed, the scientific understanding of point defects is intimately tied with the development of modern semiconductors. Intentional dopants have been probed for a wide range of applications stretching from the next generation of energy and catalytic materials in a climate-challenged society to the very quantum computers on which such materials may one day be designed on. Historically, the study of dopant technologies has largely been phenomenological in nature, due in part to the large experimental difficulty in characterizing such systems. For example, the p−n junction was discovered in 1941,[1] but a fundamental understanding of p- and n-type dopants was not provided until 1949 by Pearson and Bardeen.[2] Despite advances in computational infrastructure and refinement of quantum theory to enable widespread density functional theory (DFT) calculations, the discovery of new dopant technologies has been limited by the pace of experimental characterization with theory most useful to rationalize observed properties.

However, recent developments in the theoretical treatment of doped and defected materials aim to transform DFT from a retrospective tool to the ability to identify new defect types for a targeted application, making this an exciting time to work in the field of point defect modeling. Whether the goal is to modify the elastic, electric, or magnetic properties of a material, developing realistic and predictive computational models for such systems means tackling the perfect storm of large systems governed by complex quantum mechanical effects that lack experimental data against which to validate. Because of the wide applicability and varying critical properties of disordered materials, a disparity has emerged among theoretical descriptions of the intended use of the material. For example, computational research in energy and catalytic applications has mainly been dominated by traditional density functional calculations of fundamental material properties, such as structure, band gap, and interfacial characteristics. For these applications, there is generally a large focus on the structure and thermodynamics of the defected system.[3−5] However, describing transition-metal doping of materials for

Received: September 19, 2023
Revised: October 19, 2023
Accepted: October 20, 2023
Published: November 8, 2023

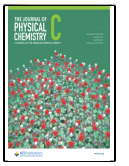

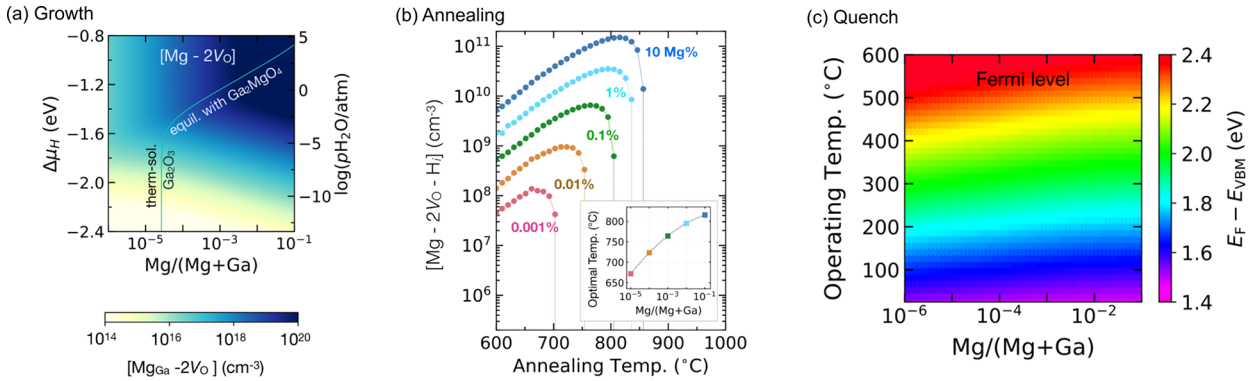

Figure 1. Predicted defect concentrations as a function of synthetic conditions predicted from first-principles calculations. An example of three-step growth−annealing−quench preparation of Mg:Ga_2O_3 is reprinted from ref 9, with the permission of AIP Publishing. (a) Defect equilibria as a function of Mg/(Mg + Ga) ratio and water vapor partial pressure (pH_2O) under the O-poor growth conditions typical for thin film growth. The solid line shows the Mg solubility limit, and the color scale shows the dopant-defect difference concentration $[Mg_{Ga} - 2V_O]$. (b) Predicted net acceptor concentration $[Mg - 2V_O - H_i]$ due to annealing. The inset shows the dependence of optimal annealing temperature on Mg concentration. (c) Predicted Fermi level ($E_F - E_{VBM}$) as a function of operating temperature and Mg doping level after quenching from the optimal temperature of the annealing step.

quantum information systems, such as qubits, has been more focused on how to calculate the electronic structure, as the performance of such systems is governed by the magneto-optical properties of the material. Predictions of the zero-field splitting,[6] hyperfine coupling,[7] and excited state properties[8] are critical, and structure is often a secondary consideration. Despite these differences, both of these fields are facing the same problems at heart: what is the balance to achieve accurate structures and properties at the same time?

This Perspective discusses recent achievements in modeling point defect systems across all potential applications to assess current best practices. We provide a consolidated resource for researchers who seek to achieve accurate geometric, thermodynamic, optical, and electronic properties simultaneously, which is critical for predicting properties for any prospective application. To ensure relevance across the entire computational materials chemistry community, we focus on results that have practical implementations and are easily generalizable for all systems. Particular emphasis is paid to advancements which replace the need for semiempirical corrections that have been prevalent in the literature and largely prevent the use of DFT as a predictive tool for defected systems. By focusing on recent and exemplary computational results, this Perspective addresses issues of model design and how to evaluate the quality of a model through the lens of current frontiers and challenges.

DESIGNING ROBUST COMPUTATIONAL MODELS

Correcting the Problems of Periodicity. Since the very first implementations of DFT, there have been two fundamental ways to represent matter. The first is as a discrete cluster with a finite number of atoms and each atomic position exactly specified; the second is through a unit cell which is then repeated by the space group operations to create an infinite lattice. While there has been some success in using cluster models to represent extended solids, it is more suited for finite structures such as molecules or nanoparticles, and thus material calculations have become dominated by the periodic supercell approach. An important consideration for the periodic approach in disordered systems is to select a supercell that is large enough to prevent artificial interactions among periodic defect images and contain the entire dopant wave function. While this problem is well-known,[10] computational expense prohibits calculations on supercells with more than approximately 1000 atoms even for basic local density approximation (LDA) approaches, which is far below typical experimental dopant loading levels.[11] Unless the computational infrastructure increases to the point where large experimentally sized unit cells can be directly calculated, the influence of the periodic boundary conditions must be considered.

Once the supercell has been built, one of the most fundamental questions to ask is: what would the equilibrium concentration of the defect be in an experimental material? For a given defect and charge state (D^q), the concentration $N(D^q)$ can be found via minimization of the total free energy of a defected system to yield

$$N(D^q) = \frac{N_{site}}{1 + g(D^q)^{-1} \exp(G_f(D^q))/k_B T} \quad (1)$$

where N_{site} and g are the number of doping sites and degeneracy, respectively, and G_f is the defect formation energy. ΔG_f is commonly defined from DFT calculation as

$$\Delta G_F = E_{DFT}(D^q) - E_{DFT}(\text{Perf}) - \sum_\alpha \Delta n^\alpha_{atom}(D^q)\mu_\alpha + q\mu_e + \Delta E_{corr} \quad (2)$$

where $E_{DFT}(D^q)$ and $E_{DFT}(\text{Perf})$ are the DFT energies of the defected and perfect unit cells, respectively, Δn_{atom} is the difference in the number of atoms of type α when the defect is formed, and ΔE_{corr} is a correction term intended to correct for finite k-point sampling or artificial periodicity of the unit cell (*vide infra*). μ_α and μ_e are the chemical potentials of atom type α and an electron, respectively. In practice, the μ_α and μ_e terms are somewhat problematic. In calculations, the former has been referenced as the total energy of the elementary phases. Experimental measurement of the latter has been difficult until recently,[12] while in calculations it has commonly been estimated as the calculated Fermi energy. However, in charged systems the correct Fermi energy would come from the maintenance of charge neutrality where the defect charge is balanced with free holes and electrons,[11] which is difficult to do using ground state DFT.

https://doi.org/10.1021/acs.jpcc.3c06267
J. Phys. Chem. C 2023, 127, 21930−21939

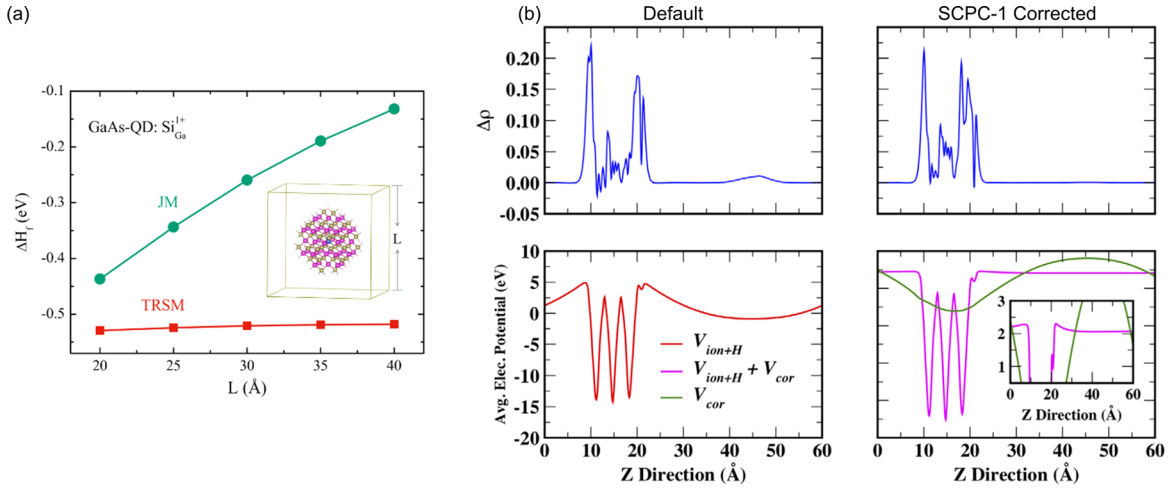

Figure 2. Charge correction schemes highly effect predicted formation energies, densities, and potentials. (a) Formation energy of a Si^+ defect in an GaAs quantum dot, with supercell length L, calculated with TRSM and traditional (JM) charge correction schemes. Reproduced with permission from ref 13. Copyright 2020 the American Physical Society. (b) Planar average of the extra charge and of the electrostatic potential along the surface normal for an O_2^- molecule on the surface of an anatase-TiO_2 (001) slab, without (Default) and with the SCPC correction. The potentials in each super cell are shown below. The corrective potential (green curve) has a Coulomb tail (highlighted in the inset) due to the negative charge on O_2, which is not removed by the correction. Reproduced with permission from ref 14. Copyright 2021 the American Physical Society.

An often overlooked point regarding DFT calculated defect concentrations is that ΔG_f is not a constant value in real systems; rather, μ_α and μ_e vary during crystal growth depending on experimental conditions like reactant ratios and thermal treatments.[15] Relative to the large number of studies that report the formation energy of defects, few have taken such effects into account. A recent example is from Goyal et al.,[9] who were able to predict H-assisted Mg doping concentrations of β-Ga_2O_3 in a three-step nonequilibrium growth−annealing−quenching process analogous to those used in the material synthesis (Figure 1). The computational results were able to suggest optimal experimental processing temperatures to achieve maximum p-type doping behavior, demonstrating the power of such calculations. The key to performing such simulations is capturing the variable chemical potential at various partial pressures of the reaction precursors. Similar approaches were also recently employed to gain insight into the oxygen vacancy concentrations of high-entropy perovskites.[16] A general framework for capturing a changing μ_α in a calculation was recently generalized by Ogawa and co-workers,[17] allowing them to reformulate the traditional constant μ_α approach as a constant concentration approach. This extends the usefulness of DFT-derived formation energies because molar ratios are controllable and measurable parameters in experiments.

As the goal of most dopant modeling is to study the defect in isolation, an important consideration for calculating defected unit cells via the supercell approach is to address the electrostatic interaction between repeated periodic charge centers. To cope with this issue, a number of correction schemes have been developed.[13,14,18,19] In general, the current standard for a charged supercell is the introduction of a compensating background jellium charge, which ensures a convergent Coulomb interaction between defect images.[18] However, this background charge has the potential to interact with the chemistry of the system, necessitating a correction scheme to fix the average electrostatic potential and total energy of the defective supercell in order to become useful. The most widely used correction schemes are all *a posteriori* in nature and do not alter the underlying wave function, merely correcting the thermodynamics with a rough approximation of the defect charge screening.[18] Such approaches are particularly troublesome for lower-dimensional materials where the charge background is distributed uniformly in the unit cell, and thus a substantial part of the counter charge is in the vacuum separating images in at least one of the three dimensions.

Recently, the problem with these uniform charge correction schemes received renewed interest, with the publication of several methods allowing for modification of the self-consistent calculation itself. Xiao et al.[13] had initially proposed their "transfer to real state" model which abandoned the jellium model. Instead, ionized electrons or holes are placed on the host band-edge states to counter the excess charge. This approach is especially intuitive for traditional semiconductors where charged defects may be compensated by electrons or holes and was shown to produce similar results to traditional charge correction schemes for bulk materials while correcting divergence for low-dimensional systems (Figure 2a).

In a different tack, da Silva et al.[14] introduced the self-consistent potential correction scheme (SCPC) which applies a corrective potential in the Kohn−Sham equations (Figure 2b). The potential includes a dielectric correction derived from an aperiodic isolated potential under open boundary conditions, which is determined in an iterative manner during the self-consistent-field (SCF) calculation. To test the utility of such an approach, they successfully calculated defect states on the hydrogenated (001) diamond surface with a nitrogen-vacancy center, where the dielectric profile of the slab was approximated by a smoothed "boxcar" function.[14] In uncorrected DFT, the negative charge of the defect artificially blue-shifts the bands of the surface states, which results in a false electronic state that can be corrected by increasing the supercell size. One potential drawback of SCPC is its reliance on the dielectric profile of the material, which is nontrivial to calculate for lower-dimensional materials.

Alternatively, the "image-charge correction" method put forth by Suo et al.[19] involves a corrective potential applied to the total electronic potential to remedy the effects of

https://doi.org/10.1021/acs.jpcc.3c06267
J. Phys. Chem. C 2023, 127, 21930−21939

periodicity. The effective potential is determined by calculation of either a perfect unit cell or a defected unit cell in the same geometry with a net neutral charge. As all defect screening information is contained within these two calculations, the problems that arise from a dielectric matrix are bypassed.

Modeling Shallow Donor Levels. Shallow defect states are defined as those that occur only within a few K_BT of the band edges. Such dopants are especially relevant for narrow band gap materials, like silicon which only provides 1.17 eV to accommodate dopant levels. Oftentimes, the dopants that create shallow levels are similar in size to the host lattice and cause minimal perturbation to the geometric and band structure. Defects of this nature are particularly desirable because they are efficient ways to introduce holes or electrons into the conduction band without the risk of recombination centers posed by deep level defects.

Obtaining an *ab initio* description of such systems poses quite a challenge due to the large supercell needed to contain the weakly bound defect state, with a hybrid functional needed to correctly localize the electron around the positively charged dopant atom. Indeed, the Coulomb interaction for such a systems only drops to 1% of its central value 54.7 Å from the center.[20] Consequently to date, the treatment of shallow impurities have mostly focused on nondensity approaches. In 2020, a DFT description of such systems was achieved by Swift and co-workers,[20] who applied a scaling method and combination of PBE and HSE06 to study the binding energy (E_b) defined as

$$E_b = \epsilon^{CB} - \epsilon^{donor} + e\Delta V \tag{3}$$

where ϵ^{CB} and ϵ^{donor} are the eigenvalues of the conduction band of a bulk supercell and occupied donor state, respectively. ΔV is a correction term corresponding to charge alignment between the bulk and impurity supercells, analogous to ΔE_{corr} in the calculation of formation energies.

By calculating the energies of a series of supercells up to 2744 atoms for PBE and 1000 atoms for HSE06, they were able to calculate the (E_b) for As and Bi doped Si very close to experimental values. Specifically, the slope (b^{fit}_{PBE}) obtained from a linear extrapolation of the PBE calculated E_b vs $1/N$, where N is the number of atoms in the supercell, was used to fit the slope for extrapolation of the HSE06 calculations (b_{HSE}) as

$$b_{HSE} = b^{fit}_{PBE} - \frac{1}{2}b^{fit}_{PBE,\delta^{ex}} + \frac{1}{2}b^{fit}_{HSE,\delta^{ex}}$$

where $b^{fit}_{PBE,\delta^{ex}}$ and $b^{fit}_{HSE,\delta^{ex}}$ were fit from the difference between the spin-up and spin-down eigenvalues (δ^{ex}) of the donor state vs $1/N$ for each supercell and were divided by 2 to yield a spin-averaged value. These slopes are intended to take into account the underestimation of electron exchange fitting from the nonhybrid PBE functional.

The final prediction of the binding energy was made by extrapolating the largest HSE06 supercell to the dilute limit based on b_{HSE}. These results are in remarkable agreement with experimental results, predicting E_b values of 54 and 67 meV for As and Bi donors, with the experimental data at 53.9 and 70.9 meV.[20] Similar extrapolations were made to successfully calculate the hyperfine and superhyperfine interactions of such dopants. In a similar nature, Liu et al.[21] recently developed a scaling method to extrapolate the formation energies and charge transition levels of point defects in hexagonal boron nitride.

Choosing an Accurate and Efficient Basis Set. Despite the tremendous success of such scaling approaches to accurately capture the properties of experimental systems, it is critical to note that the supercells needed to obtain linear scaling are still beyond what is accessible to most researchers for many systems of interest. Indeed, Swift et al. reported that a typical Kohn−Sham SCF cycle took approximately 96 h on 60 cores for the HSE calculations with 1000 atoms.[20] Thus, continued effort to determine exactly what levels of theory are needed to calculate the properties of such systems is critical.

In particular, the use of plane wave versus atom-centered basis sets to describe extended solids or defects remains one of the most important yet underexamined problems in computational chemistry. The role of pseudopotentials (PPs) to describe the interaction between core and valence electrons is still up for debate, and has been gaining increased attention in the quantum materials community as calculation of the Fermi contact contribution to the hyperfine splitting requires an accurate spin density exactly at the high spin nucleus.[22] Some insight into the problem was recently provided by Ghosh et al.,[22] who used a real-space mixed all-electron (AE) PP approach to calculate spin Hamiltonian parameters of two qubit systems. Their results indicated that reasonable hyperfine parameters can be achieved if the all-electron scheme is applied to only a few atoms around the defect (e.g., around 10). Such results will be particularly useful with the continued emergence of embedding schemes, in which the defect orbitals are calculated with a higher level of theory than the host lattice.[23]

From a more practical standpoint, constructing the all-electron charge density from PPs using the projector augmented wave (PAW) method has been shown to be successful in calculating the hyperfine parameters of some transition-metal-doped systems.[24] A comparison between the different approaches was attempted by Ma et al.[25] in 2022. Calculated hyperfine parameters for shallow dopant systems using the PP-PAW method in VASP[26,27] and AE and PP-AE in CP2K[28] were compared. However, unlike the linear fitting scheme employed by Swift et al.,[20] Ma et al.[25] opted instead for a quadratic fit yielding extrapolated hyperfine values of 56.7, 115.5, and 112.5 MHz (exp = 117 MHz) for the PP-PAW, AE, and PP-AE approaches, respectively. Of note is the decreased computational scaling of the atom-centered approach in CP2K, enabling calculations on supercells up to 4096 atoms versus 1000 atoms for the PP-PAW approach.[25] Clearly, the discrepancies in expense and predicted properties between the two approaches warrant further benchmarking to understand the ability of each to describe different material types and particular material properties.

Optimizing to a Representative Structure. Often dopant geometries are calculated in isolation as idealized structures, as including real crystal features like other defects and interfaces is nontrivial. Thus, standard practice for dopant modeling is to begin with a pure crystal representation of the host material and insert the dopant atom at either a substitutional or an interstitial site.[8−10,24] In principle, this idealized structure can then be optimized to the lowest energy configuration.

The largest issue for typical decent optimizers is that these materials have many local minima due to the large number of atoms, and starting from a fairly low energy bulk geometry with only slight defects added does not provide large force on the

https://doi.org/10.1021/acs.jpcc.3c06267
J. Phys. Chem. C 2023, 127, 21930−21939

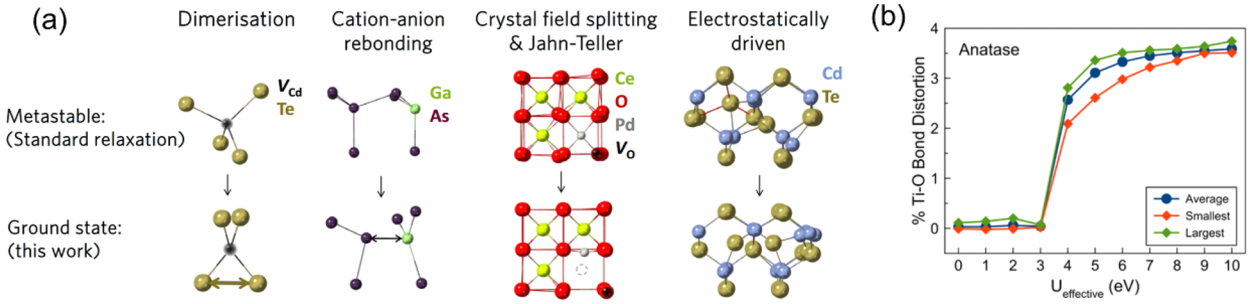

Figure 3. Calculated geometries dependent on initial guess (a) and optimization parameters (b). (a) Examples of symmetry-breaking reconstructions at point defect sites: dimerization, cation−anion rebonding, crystal field splitting, and Jahn−Teller, and electrostatically driven, found in both high-symmetry (metastable) and symmetry-broken (ground state) optimization schemes. Reprinted from ref 29 under the Creative Commons license. (b) Representative Ti−O bond elongations (% distortions relative to bulk neutral anatase TiO_2) around Ti polaronic sites optimized with different U values. Reproduced with permission from ref 30.

atoms early in the optimization. Thus, a common pitfall is optimizing to a local rather than global minimum by using standard DFT methods. Alternative approaches, such as that proposed by Arrigoni and Madsen,[31] that utilize an evolutionary algorithm to find low-energy defect configurations, are appealing for in-depth studies of single defects, but because of their computational cost and poor generalizability, they have not become a standard approach. Therefore, increased research is needed to understand how to best use the optimizers that are currently widely available.

Mosquera-Lois and co-workers[29] have recently called attention to this issue specifically in the arena of discovering new defect geometries. By using a set of eight crystallographically distinct materials with different point defects, they showed that traditional geometry optimization would predict incomplete minimization of defect structures in all cases (Figure 3a). To address this, the authors proposed random displacements of each atom in the unit cell prior to the traditional geometry optimization. These "rattled" structures allowed the optimizer to escape local minima and relax to a lower energy ground state structure. Such symmetry breaking has been shown to improve the optimization behavior in TiO_2 nanoparticles previously.[32] As a general rule of thumb, it was suggested that structural perturbations of around −40% to +20% to provide optimal results.[29]

In addition to random atomic perturbations, systematic modification of the starting geometry also has the potential to alter the optimization pathway. Few communities have done as much to take advantage of this fact than those modeling polarons.[30] A polaron is defined as an electron localized within a well created by the displaced ions that surround it. Indeed, the localized orbitals around a dopant atom would be considered a special case of polaron. However, some materials also have a propensity to form self-trapped polarons in the pure phase through electron−phonon coupling processes.[33] Capturing such excited states in DFT optimizations without altering the underlying calculation, such as direct control of the occupation matrices,[34] requires a careful touch and is something of an art. Polaron approaches can be applied to the cases of dopant sites where localized charge is targeted, even in cases in which traditional density functionals would relax to an alternate solution.

A comparison of different methods to creating a localized charge state in three different materials was presented by Pham and Deskins in 2020.[30] The most efficient approach involves artificially lengthening the bonds around a dopant atom to encourage localization. By using this "excited" state geometry as the guess for geometry optimization, it was shown that polaron localization can be controlled to specific lattice sites. An approximately 4% bond lengthening was found to be the optimal elongation distance to create both the polaron and minimizing the number of optimizations steps.[30]

In a similar vein, a wave function with the appropriately localized charge density can be used as an initial guess to bias the optimization. Such is easily accomplished through a more aggressive approach of using large Hubbard U values on the target site (Figure 3b).[30] In this scenario, the advisable approach would be to use the large U value in initial optimization steps and then reduce it over the course of the optimization until $U = 0$, leading to localization that can be controlled by the optimization procedure. This is especially critical due to the feedback loop that exists between geometric and electronic structure. The applicability of such approaches needs to be closely scrutinized to ensure that physical results are achieved without simply biasing the system via tunable parameters.

EVALUATING THE QUALITY OF A MODEL

Koopman's Compliance for Tuned Functionals. Even high-quality functionals use parametrization. In particular, hybrids, such as HSE06 and PBE0, have an α parameter, which specifies the amount of exact exchange (HSE06 also possesses a range separation parameter). In the default configurations, each of these functionals mixes 25% exact Hartree−Fock exchange (i.e., $\alpha = 0.25$). Recently, there has been increased attention to adjust this parameter in material specific ways in order to better capture experimental properties.[35] While picking the optimal α value has been accomplished in various ways, for example by matching to experimental band gaps, a theoretically justified α must satisfy the generalized Koopman's condition.

Many wave functions and densities are solved using the fact that the exact total energy of a many-electron system is piecewise linear with respect to the number of electrons n. A convenient way to ensure this linearity of a DFT functional is given by the generalized Koopman's condition

$$-I(n+1) \equiv E(n+1) - E(n) = \epsilon_{n+1}(n+1) \quad (4)$$

where $I(n)$ and $E(n)$ are the ionization and total energy of an n electron system, and ϵ_i denotes the ith eigenvalue of an n-electron system. While such an approach only describes the occupied orbitals in a system, the benefit of fitting functional

https://doi.org/10.1021/acs.jpcc.3c06267
J. Phys. Chem. C 2023, 127, 21930−21939

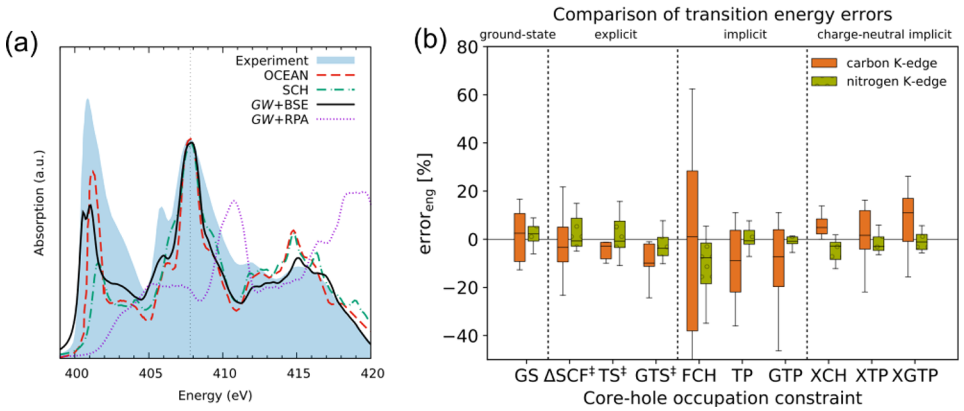

Figure 4. Predicting X-ray analysis parameters that can be directly compared to experiment. (a) Comparison of experiment[47] with supercell core−hole (SCH)[48] and Green's function (GW), Bethe−Salpeter (BSE), OCEAN,[49] and random-phase approximation (RPA) methods for predicting the XAS K edge of N in h-BN. Reproduced with permission from ref 48. Copyright 2022 American Physical Society. (b) Transition energy error box plots for core−hole occupation constraining approaches. The median (horizontal line), interquartile range (IQR, box outlining the 75% and 25% percentiles), and maximum absolute errors (MAEs, shown as error bars at the 99% and 1% percentiles) are provided to quantify the precision and accuracy of each method. Reproduced with permission from ref 50. Copyright 2019 AIP Publishing.

parameters this way as opposed to improving materials descriptions with DFT+U methods is that better functionals often describe all materials properties well at the same time, whereas DFT+U will often describe one property correctly and another incorrectly.[36]

Despite the increasing awareness of the need to tailor α in materials calculations in recent years, determining Koopman's compliance necessitates many trial calculations on the same system using expensive hybrid functionals. Alternative methods have been proposed for determining α based on the dielectric constant of the material.[37] Yang and Pasquerello[38] recently proposed a method for calculating α, which takes advantage of the Koopman's assured condition that the energy level of a defect state should remain constant regardless if it is occupied or unoccupied. To determine the optimal α for a material, this approach involves inserting either a tunable point charge or Gaussian charge distribution into the largest interstitial site available in the crystal to introduce defect states that can be either occupied or unoccupied. Because these defect levels evolve linearly with α, the occupied or unoccupied defect levels can be extrapolated to where they intersect, yielding a fitted α. In cases where semilocal functionals are able to predict a somewhat reasonable defect level, the procedure can be accomplished in a "one-shot" fashion, where the defect energy levels are obtained by applying hybrid-functional Hamiltonian to the GGA-calculated wave functions. Selection of the screening parameter for range-separated functional was accomplished by Yang et al.,[39] who derived an expression for an optimal value based on a function of the short-range and long-range Fock exchange fractions.

Despite these advances, it remains difficult to use such approaches to model metal-atom-doped systems because it is not guaranteed that a parametrized α for a host lattice will correctly describe the doped system properly. Additionally, issues arise when defect states lie close to a band edge and complicate the application of Koopman's theorem. Furthermore, this approach only considers the occupied orbitals, and a correct description of many complicated transition-metal point defects requires consideration of virtual orbitals as well. Thus, further investigation and improved methods of functional fitting for doped systems should be developed.

Comparing between Theory and Experiment. While Koopman's theorem provides a prescription for obtaining functionals that are theoretically sound, there is no guarantee that the tuned functional will reproduce the experimental properties. Therefore, the need to compare to experimental observables remains. Furthermore, one of the major appeals of computational materials chemistry is the deconvolution of experimental spectra. Fortunately, much of the theory for translating between Kohn−Sham calculated densities and experimental observables has already been developed.[11] Hence, progress is governed almost universally by the ability of a chosen basis set and functional to accurately capture the properties of a real material. Indeed, recent exemplary insights into experimental data by comparison to DFT are far too numerous to capture in a single publication. However, scanning tunneling microscopy and spectroscopy,[40−42] vibrational properties,[43] electron paramagnetic and nuclear magnetic resonance, Mössbauer spectroscopy,[24,44,45] and transport and optical properties[46] are amenable to comparison with experiment. Computational studies should begin reporting these values to evaluate the quality of a computational model and to provide direct comparison to experiment.

Improvements in the Prediction of X-ray Spectroscopy. X-ray adsorption fine structure (XAFS) and X-ray photoelectron spectroscopy (XPS) provide important information about the crystal structure surrounding a defect. Both methods rely on excitation of a core level electron but differ in that the measurement of XAFS is absorption to a higher excited state as a function of X-ray energy, while XPS measures the kinetic energy of electrons ejected from the material at constant laser potential. First-principles calculation of these spectra for solids is afflicted by a lack of high quality description of core electron levels and, in the case of XAFS, failing to appropriately treat the excited electron.[51]

Much effort has been recently devoted to obtaining a high quality description of the core−hole system using DFT.[51] A basic technique involves manually enforcing the core−hole electron configuration and then performing an SCF calculation to relax the rest of the system around this constraint to yield an excited state energy as

https://doi.org/10.1021/acs.jpcc.3c06267
J. Phys. Chem. C 2023, 127, 21930−21939

$$\Delta E_{\Delta SCF} = E_F - E_i = E(q_c b = 0, q_v b = 1) - E(q_c b = 1, q_v b = 0) \quad (5)$$

where E is the total energy and q_{cb} and q_{vb} are the occupation of the core level and valence band, respectively. This basic approach, termed ΔSCF, was examined in the context of all-electron periodic solids in 2021 by Kahk et al.,[52] who found excellent agreement between the experimental and calculated binding energies with a mean error of 0.24 eV for all systems considered. Furthermore, the ability to use the ΔSCF method to model the ground state in high-spin metals was recently examined.[53] Indeed, a variant of the ΔSCF approach such known as the supercell core−hole method (SCH) has been recently implemented into VASP to allow computation of XAFS spectra with accuracy similar to that of higher level Green's function and screened Coulomb interaction (GW) methods (Figure 4a).[48]

Despite these successes, variational collapse to the ground state and oscillatory convergence are common occurrences in ΔSCF calculations.[51] Furthermore, the construction of a full XAFS spectrum would require many calculations to describe every possible $i \rightarrow j$ transition. As a result, many modifications have been proposed to the ΔSCF method. Some of these alter the occupation of the core state without altering that of the virtual orbitals.[51] This essentially minimizes the contribution of the excited state electron, enabling a single SCF calculation to obtain the transition energies to different unoccupied Kohn−Sham states. The excess charge created by such approaches has been dealt with in methods such as the excited electron and core−hole (XCH) approach,[54] which places the electron in the LUMO only but references the energies of all virtual Kohn−Sham orbitals. Several recent insights into materials properties have been gained using the XCH approach, including probing the electric-field-induced doping mechanism in $YBa_2Cu_3O_7$.[55] A comparison of the different ΔSCF flavors was performed by Michelitsh and Reuter[50] (Figure 4b), who demonstrated that semiquantitative analysis of experimental data can be obtained at the semilocal level of density functionals. While the ΔSCF approach has indeed proven valuable in approximating the absorption properties of materials, a more rigorous theoretical treatment of excitonic properties would necessarily invoke the GW methods with the Bethe−Salpeter equation. However, the significantly higher computational cost of such approaches necessitates smaller unit cells, which in turn also compromises the quality of a calculation.

FRONTIERS

A particularly promising approach to combine the accuracy of wave function methods with the affordability of DFT calculations is embedding approaches. These calculations involve treating a small region (e.g., the dopant or defect) with an accurate but expensive level of theory, while the remainder of the system is treated with a DFT or Hartree−Fock description. Many different flavors for such embedding potentials have evolved in recent years.[23,56−58] The challenges to such approaches, occurring in most of the implementations, are deciding which orbitals to treat at the higher level of theory, known as the active space (Figure 5), and determining how to describe the interface region between the different levels of theory. The need to decide these and other model parameters significantly limits the use of such methods in an *ab initio* capacity, requiring a significant prerequisite knowledge of the system and targeted chemistry. Furthermore, any quantum embedding approach for materials has yet to be distributed in a widely available software package, which severely limits widespread application and the number of systems tested. For these reasons, embedding schemes will likely remain specialized approaches to obtain extremely detailed electronic information on known interesting defects.

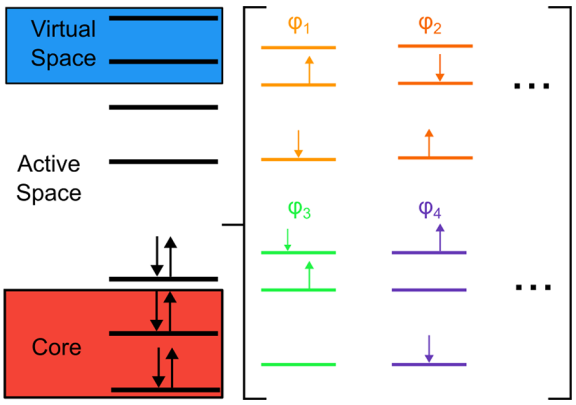

Figure 5. Representative active space for a metal ion dopant and configuration interaction-like expansion needed to represent its electronic structure in an embedding scheme.

In addition, while embedding methods can provide a highly accurate picture of the static properties of an excited system, further advancements are needed to understand the time domain of excited properties. Notable work in this area has been accomplished by Akimov and Prezhdo, who introduced the Python extension for *ab initio* dynamics (PYXAID)[60] providing an accessible way to perform nonadiabatic molecular dynamics simulations in extended systems. The software works by combining surface hopping approaches with real-time TD-DFT and interfacing it with multiple quantum chemistry codes. This work represents a significant achievement for materials modeling, as the majority of other theoretical advancements in this area have been exclusive to molecular systems. The implementation of PYXAID is made computationally feasible through the use of classical path approximation (CPA), which neglects the effect of different electronic states on nuclear geometry. This approach has led to a number of notable insights into the time scales of processes in doped materials[59,61−63] (Figure 6). A critical limitation of CPA is that nuclear structural reorganizations, such as bond breaking and formation, cannot be studied. Furthermore, the quality of the derived electronic structures remains dependent on the underlying density functional, and the current method is limited to only the most computationally efficient LDA and generalized gradient approximation (GGA) approaches. Likely, such issues will not be resolved until the adoption of more powerful computers or algorithms capable of operating without the constraints of CPA or computationally efficient pure density functionals.

OUTLOOK

The past half-decade has seen remarkable advancements in the study of point defects. For much of this time, theory has played a retrospective role in rationalizing observational experimental results. Recent advances in DFT make it possible to obtain a realistic representation of all material properties simultaneously in an entirely *ab initio* approach. These new methods have the

https://doi.org/10.1021/acs.jpcc.3c06267
J. Phys. Chem. C 2023, 127, 21930−21939

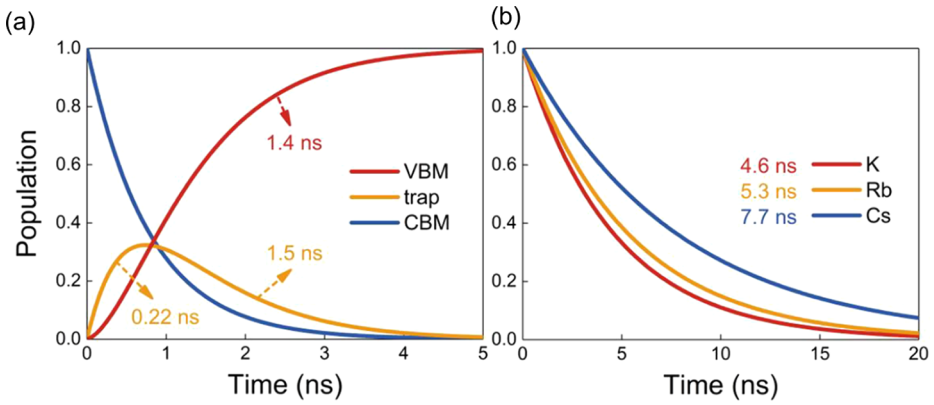

Figure 6. Insights into charge relaxation obtained from surface hopping methods. Nonradiative charge relaxation dynamics in $MAPb_0.5Sn_0.5I_3$ (a) containing V_Sn and (b) V_Sn doped with an alkali metal: K, Rb, and Cs. The time scales of both holes and electrons are predicted, along with trap-assisted and direct recombination. Reproduced in part with permission from ref 59.

potential to transform computation into a predictive tool with the ability to identify and screen new dopants and materials.

The predictive success of DFT will also require adjustments to the current paradigm for point defect modeling. For example, much effort has been spent on modeling dopants in isolation. However, real material properties are the result of an ensemble of disorder, and effects such as defect aggregation, charge compensation complexes, and defect migration are critical research areas for the computational materials chemistry community to tackle in the future. Furthermore, methods to study the interdependence of properties (e.g., electron−phonon coupling or nonadiabatic dynamics) are critical to obtaining experimentally relevant materials models. It is expected that these developments will coincide with modeling improvements like those presented in this Perspective, ultimately allowing highly accurate calculation of material properties in an affordable manner.

AUTHOR INFORMATION

Corresponding Author

Lisa A. Fredin − *Department of Chemistry, Lehigh University, Bethlehem, Pennsylvania 18015, United States;* orcid.org/0000-0002-4091-0899; Email: lafredin@lehigh.edu

Author

Gil M. Repa − *Department of Chemistry, Lehigh University, Bethlehem, Pennsylvania 18015, United States*

Complete contact information is available at: https://pubs.acs.org/10.1021/acs.jpcc.3c06267

Notes

The authors declare no competing financial interest.

Biographies

Gil M. Repa received his B.S. in Biochemistry from Oklahoma State University. He is pursuing a PhD in Chemistry at Lehigh University under the mentorship of Lisa A. Fredin. His research draws on experience using a combination of density functional theory and classical molecular mechanics to develop an understanding of the structure−function relationship of materials. He is particularly interested in developing accurate and generalizable models for a range of structurally disordered systems.

Lisa A. Fredin is an Assistant Professor of Chemistry at Lehigh University. Her research draws on her background, combining experiment and theory to develop computational and theoretical models of fundamental electronic properties to design materials with targeted properties. The Fredin group develops models of the chemistry and physics of a broad range of disordered materials, bridging physical chemistry, material science, nanoscience, and computation, as well as probing the boundaries of the particle and wave approximations of electrons in materials. Prof. Fredin earned a doctorate in chemistry at Northwestern University and a bachelor's in chemistry, biochemistry, and applied mathematics (minor in computer science) at the University of Texas at Austin. Before coming to Lehigh, Fredin served as a research chemist at the National Institute of Standards and Technology in Gaithersburg, MD.

ACKNOWLEDGMENTS

We acknowledge financial support from Lehigh University and by the NSF Chemical Structure, Dynamics, and Mechanisms A Program under award number CHE-2310205. Research computing resources provided by Lehigh University partially supported by the NSF CC* Compute program through OAC-2019035 and the TG-CHE190011 allocation from Extreme Science and Engineering Discovery Environment (XSEDE),[64] which is supported by National Science Foundation Grant ACI-1548562, are also acknowledged.

REFERENCES

(1) Riordan, M.; Hoddeson, L. The origins of the pn junction. *IEEE Spectrum* **1997**, *34*, 46−51.

(2) Pearson, G. L.; Bardeen, J. Electrical Properties of Pure Silicon and Silicon Alloys Containing Boron and Phosphorus. *Phys. Rev.* **1949**, *75*, 865−883.

(3) Brimley, P.; Almajed, H.; Alsunni, Y.; Alherz, A. W.; Bare, Z. J. L.; Smith, W. A.; Musgrave, C. B. Electrochemical CO_2 Reduction over Metal-/Nitrogen-Doped Graphene Single-Atom Catalysts Modeled Using the Grand-Canonical Density Functional Theory. *ACS Catal.* **2022**, *12*, 10161−10171.

(4) Dhandapani, H. N.; Mahendiran, D.; Karmakar, A.; Devi, P.; Nagappan, S.; Madhu, R.; Bera, K.; Murugan, P.; Babu, B. R.; Kundu, S. Boosting of overall water splitting activity by regulating the electron distribution over the active sites of Ce doped NiCo−LDH and atomic level understanding of the catalyst by DFT study. *J. Mater. Chem. A* **2022**, *10*, 17488−17500.

(5) Zhou, S.; Wan, Q.; Lin, S.; Guo, H. Acetylene hydrogenation catalyzed by bare and Ni doped CeO_2 (110): the role of frustrated Lewis pairs. *Phys. Chem. Chem. Phys.* **2022**, *24*, 11295−11304.

(6) Mondal, S.; Lunghi, A. Spin-phonon decoherence in solid-state paramagnetic defects from first principles. *npj Comput. Mater.* **2023**, *9*, 120.

(7) Körner, W.; Ghassemizadeh, R.; Urban, D. F.; Elsässer, C. Influence of (N,H)-terminated surfaces on stability, hyperfine structure, and zero-field splitting of NV centers in diamond. *Phys. Rev. B* **2022**, *105*, 085305.
(8) Shang, L.; Chen, Q.; Jing, W.; Ma, C.-G.; Duan, C.-K.; Du, J. First-principles study of transition metal dopants as spin qubits. *Phys. Rev. Mater.* **2022**, *6*, 086201.
(9) Goyal, A.; Zakutayev, A.; Stevanović, V.; Lany, S. Computational Fermi level engineering and doping-type conversion of Mg:Ga_2O_3 via three-step synthesis process. *J. Appl. Phys.* **2021**, *129*, 245704.
(10) Repa, G. M.; Fredin, L. A. Parameter space exploration reveals interesting Mn-doped $SrTiO_3$ structures. *Phys. Chem. Chem. Phys.* **2021**, *23*, 23486−23500.
(11) Freysoldt, C.; Grabowski, B.; Hickel, T.; Neugebauer, J.; Kresse, G.; Janotti, A.; Van De Walle, C. G. First-principles calculations for point defects in solids. *Rev. Mod. Phys.* **2014**, *86*, 253−305.
(12) Yang, F.; Zibrov, A. A.; Bai, R.; Taniguchi, T.; Watanabe, K.; Zaletel, M. P.; Young, A. F. Experimental Determination of the Energy per Particle in Partially Filled Landau Levels. *Phys. Rev. Lett.* **2021**, *126*, 156802.
(13) Xiao, J.; Yang, K.; Guo, D.; Shen, T.; Deng, H.-X.; Li, S.-S.; Luo, J.-W.; Wei, S.-H. Realistic dimension-independent approach for charged-defect calculations in semiconductors. *Phys. Rev. B* **2020**, *101*, 165306.
(14) Chagas Da Silva, M.; Lorke, M.; Aradi, B.; Farzalipour Tabriz, M.; Frauenheim, T.; Rubio, A.; Rocca, D.; Deák, P. Self-Consistent Potential Correction for Charged Periodic Systems. *Phys. Rev. Lett.* **2021**, *126*, 076401.
(15) Khlyustova, A.; Sirotkin, N.; Kusova, T.; Kraev, A.; Titov, V.; Agafonov, A. Doped TiO_2: the effect of doping elements on photocatalytic activity. *Materials Advances* **2020**, *1*, 1193−1201.
(16) Park, J.; Xu, B.; Pan, J.; Zhang, D.; Lany, S.; Liu, X.; Luo, J.; Qi, Y. Accurate prediction of oxygen vacancy concentration with disordered A-site cations in high-entropy perovskite oxides. *npj Comput. Mater.* **2023**, *9*, 29.
(17) Ogawa, T.; Taguchi, A.; Kuwabara, A. An extended computational approach for point-defect equilibria in semiconductor materials. *npj Comput. Mater.* **2022**, *8*, 79.
(18) Makov, G.; Payne, M. C. Periodic boundary conditions in *ab initio* calculations. *Phys. Rev. B* **1995**, *51*, 4014−4022.
(19) Suo, Z.-J.; Luo, J.-W.; Li, S.-S.; Wang, L.-W. Image charge interaction correction in charged-defect calculations. *Phys. Rev. B* **2020**, *102*, 174110.
(20) Swift, M. W.; Peelaers, H.; Mu, S.; Morton, J. J. L.; Van De Walle, C. G. First-principles calculations of hyperfine interaction, binding energy, and quadrupole coupling for shallow donors in silicon. *npj Comput. Mater.* **2020**, *6*, 181.
(21) Liu, X.; Gao, Z.; Wang, V.; Luo, Z.; Lv, B.; Ding, Z.; Zhang, Z. Extrapolated Defect Transition Level in Two-Dimensional Materials: The Case of Charged Native Point Defects in Monolayer Hexagonal Boron Nitride. *ACS Appl. Mater. Interfaces* **2020**, *12*, 17055−17061.
(22) Ghosh, K.; Ma, H.; Onizhuk, M.; Gavini, V.; Galli, G. Spin−spin interactions in defects in solids from mixed all-electron and pseudopotential first-principles calculations. *npj Comput. Mater.* **2021**, *7*, 123.
(23) Pfäffle, W.; Antonov, D.; Wrachtrup, J.; Bester, G. Screened configuration interaction method for open-shell excited states applied to NV centers. *Phys. Rev. B* **2021**, *104*, 104105.
(24) Repa, G. M.; Fredin, L. A. Mn environment in doped $SrTiO_3$ revealed by first-principles calculation of hyperfine splittings. *Appl. Phys. Lett.* **2022**, *121*, 022401.
(25) Ma, H.; Hsueh, Y.-L.; Monir, S.; Jiang, Y.; Rahman, R. Ab-initio calculations of shallow dopant qubits in silicon from pseudopotential and all-electron mixed approach. *Commun. Phys.* **2022**, *5*, 165.
(26) Blöchl, P. E. Projector augmented-wave method. *Phys. Rev. B* **1994**, *50*, 17953−17979.
(27) Kresse, G.; Furthmüller, J. Efficient iterative schemes for *ab initio* total-energy calculations using a plane-wave basis set. *Phys. Rev. B* **1996**, *54*, 11169−11186.
(28) Kühne, T. D.; Iannuzzi, M.; Del Ben, M.; Rybkin, V. V.; Seewald, P.; Stein, F.; Laino, T.; Khaliullin, R. Z.; Schütt, O.; Schiffmann, F.; et al. CP2K: An electronic structure and molecular dynamics software package - Quickstep: Efficient and accurate electronic structure calculations. *J. Chem. Phys.* **2020**, *152*, 194103.
(29) Mosquera-Lois, I.; Kavanagh, S. R.; Walsh, A.; Scanlon, D. O. Identifying the ground state structures of point defects in solids. *npj Comput. Mater.* **2023**, *9*, 25.
(30) Pham, T. D.; Deskins, N. A. Efficient Method for Modeling Polarons Using Electronic Structure Methods. *J. Chem. Theory Comput.* **2020**, *16*, 5264−5278.
(31) Arrigoni, M.; Madsen, G. K. H. Evolutionary computing and machine learning for discovering of low-energy defect configurations. *npj Comput. Mater.* **2021**, *7*, 71.
(32) Repa, G. M.; Fredin, L. A. Capturing experimental properties in computationally efficient faceted titania nanoparticle models. *Int. J. Quantum Chem.* **2023**, *123*, 123.
(33) Franchini, C.; Reticcioli, M.; Setvin, M.; Diebold, U. Polarons in materials. *Nat. Rev. Mater.* **2021**, *6*, 560−586.
(34) Chai, Z.; Teobaldi, G.; Si, R.; Liu, L.-M. Subspace Occupancy-Constraining Potentials for Modeling Polaron Formation. *J. Phys. Chem. C* **2021**, *125*, 26354−26362.
(35) Elmaslmane, A. R.; Wetherell, J.; Hodgson, M. J. P.; McKenna, K. P.; Godby, R. W. Accuracy of electron densities obtained via Koopmans-compliant hybrid functionals. *Phys. Rev. Mater.* **2018**, *2*, 040801.
(36) Falletta, S.; Pasquarello, A. Hubbard U through polaronic defect states. *npj Comput. Mater.* **2022**, *8*, 263.
(37) Cipriano, L. A.; Di Liberto, G.; Tosoni, S.; Pacchioni, G. Band Gap in Magnetic Insulators from a Charge Transition Level Approach. *J. Chem. Theory Comput.* **2020**, *16*, 3786−3798.
(38) Yang, J.; Falletta, S.; Pasquarello, A. One-Shot Approach for Enforcing Piecewise Linearity on Hybrid Functionals: Application to Band Gap Predictions. *J. Phys. Chem. Lett.* **2022**, *13*, 3066−3071.
(39) Yang, J.; Falletta, S.; Pasquarello, A. Range-separated hybrid functionals for accurate prediction of band gaps of extended systems. *npj Comput. Mater.* **2023**, *9*, 108.
(40) Spera, M.; Scarfato, A.; Pásztor, Á.; Giannini, E.; Bowler, D.; Renner, C. Insight into the Charge Density Wave Gap from Contrast Inversion in Topographic STM Images. *Phys. Rev. Lett.* **2020**, *125*, 267603.
(41) Wyrick, J.; Wang, X.; Namboodiri, P.; Kashid, R. V.; Fei, F.; Fox, J.; Silver, R. Enhanced Atomic Precision Fabrication by Adsorption of Phosphine into Engineered Dangling Bonds on H−Si Using STM and DFT. *ACS Nano* **2022**, *16*, 19114−19123.
(42) Herrera-Reinoza, N.; Dos Santos, A. C.; De Lima, L. H.; Landers, R.; De Siervo, A. Atomically Precise Bottom-Up Synthesis of h-BNC: Graphene Doped with h-BN Nanoclusters. *Chem. Mater.* **2021**, *33*, 2871−2882.
(43) Kou, Z.; Hashemi, A.; Puska, M. J.; Krasheninnikov, A. V.; Komsa, H.-P. Simulating Raman spectra by combining first-principles and empirical potential approaches with application to defective MoS2. *npj Computat. Mater.* **2020**, *6*, 59.
(44) Komedera, K.; Gatlik, J.; Błachowski, A.; Zukrowski, J.; Sato, T. J.; Legut, D.; Wdowik, U. D. Mössbauer studies of spin and charge modulations in $BaFe_2$ (As 1 x P x) 2. *Phys. Rev. B* **2021**, *103*, 024526.
(45) Liu, Y.; Lan, R.; Dong, C.; Wang, K.; Fu, X.; Liu, H.; Qian, Y.; Wang, J. High-Temperature Magic-Angle Spin Nuclear Magnetic Resonance Reveals Sodium Ion-Doped Crystal-Phase Formation in FLiNaK Eutectic Salt Solidification. *J. Phys. Chem. C* **2021**, *125*, 4704−4709.
(46) Guziewicz, E.; Volnianska, O.; Demchenko, I.; Zeller, P.; Amati, M.; Gregoratti, L. Valence-Band Electronic Structure of ZnO and ZnO:N: Experimental and Theoretical Evidence of Defect Complexes. *Physical Review Applied* **2022**, *18*, 044021.

https://doi.org/10.1021/acs.jpcc.3c06267
J. Phys. Chem. C 2023, 127, 21930−21939

(47) Petravic, M.; Peter, R.; Varasanec, M.; Li, L. H.; Chen, Y.; Cowie, B. C. C. Vibronic fine structure in high-resolution x-ray absorption spectra from ion-bombarded boron nitride nanotubes. *Journal of Vacuum Science & Technology A: Vacuum, Surfaces, and Films* **2013**, *31*, 031405.
(48) Unzog, M.; Tal, A.; Kresse, G. X-ray absorption using the projector augmented-wave method and the Bethe-Salpeter equation. *Phys. Rev. B* **2022**, *106*, 155133.
(49) Gilmore, K.; Vinson, J.; Shirley, E.; Prendergast, D.; Pemmaraju, C.; Kas, J.; Vila, F.; Rehr, J. Efficient implementation of core-excitation Bethe−Salpeter equation calculations. *Comput. Phys. Commun.* **2015**, *197*, 109−117.
(50) Michelitsch, G. S.; Reuter, K. Efficient simulation of near-edge x-ray absorption fine structure (NEXAFS) in density-functional theory: Comparison of core-level constraining approaches. *J. Chem. Phys.* **2019**, *150*, 074104.
(51) Besley, N. A. Modeling of the spectroscopy of core electrons with density functional theory. *WIREs Comput. Mol. Sci.* **2021**, *11*, No. e1527.
(52) Kahk, J. M.; Michelitsch, G. S.; Maurer, R. J.; Reuter, K.; Lischner, J. Core Electron Binding Energies in Solids from Periodic All-Electron -Self-Consistent-Field Calculations. *J. Phys. Chem. Lett.* **2021**, *12*, 9353−9359.
(53) Bagus, P. S.; Nelin, C. J.; Brundle, C. R.; Crist, B. V.; Lahiri, N.; Rosso, K. M. Combined multiplet theory and experiment for the Fe 2p and 3p XPS of FeO and Fe_2O_3. *J. Chem. Phys.* **2021**, *154*, 094709.
(54) Prendergast, D.; Galli, G. X-Ray Absorption Spectra of Water from First Principles Calculations. *Phys. Rev. Lett.* **2006**, *96*, 215502.
(55) Poloni, R.; Mariano, A. L.; Prendergast, D.; Garcia-Barriocanal, J. Probing the electric field-induced doping mechanism in YBa2Cu3O7 using computed Cu K-edge x-ray absorption spectra. *J. Chem. Phys.* **2018**, *149*, 234706.
(56) Mitra, A.; Pham, H. Q.; Pandharkar, R.; Hermes, M. R.; Gagliardi, L. Excited States of Crystalline Point Defects with Multireference Density Matrix Embedding Theory. *J. Phys. Chem. Lett.* **2021**, *12*, 11688−11694.
(57) Muechler, L.; Badrtdinov, D. I.; Hampel, A.; Cano, J.; Rösner, M.; Dreyer, C. E. Quantum embedding methods for correlated excited states of point defects: Case studies and challenges. *Phys. Rev. B* **2022**, *105*, 235104.
(58) Sheng, N.; Vorwerk, C.; Govoni, M.; Galli, G. Green's Function Formulation of Quantum Defect Embedding Theory. *J. Chem. Theory Comput.* **2022**, *18*, 3512−3522.
(59) Shi, R.; Long, R. Atomic Model for Alkali Metal-Doped Tin−Lead Mixed Perovskites: Insight from Quantum Dynamics. *J. Phys. Chem. Lett.* **2023**, *14*, 2878−2885.
(60) Akimov, A. V.; Prezhdo, O. V. The PYXAID Program for Non-Adiabatic Molecular Dynamics in Condensed Matter Systems. *J. Chem. Theory Comput.* **2013**, *9*, 4959−4972.
(61) Shi, R.; Fang, Q.; Vasenko, A. S.; Long, R.; Fang, W.-H.; Prezhdo, O. V. Structural Disorder in Higher-Temperature Phases Increases Charge Carrier Lifetimes in Metal Halide Perovskites. *J. Am. Chem. Soc.* **2022**, *144*, 19137−19149.
(62) Zhao, X.; Vasenko, A. S.; Prezhdo, O. V.; Long, R. Anion Doping Delays Nonradiative Electron−Hole Recombination in Cs-Based All-Inorganic Perovskites: Time Domain ab Initio Analysis. *J. Phys. Chem. Lett.* **2022**, *13*, 11375−11382.
(63) Katin, K. P.; Maslov, M. M.; Nikitenko, V. R.; Kochaev, A. I.; Kaya, S.; Prezhdo, O. V. Anisotropic Carrier Mobility and Spectral Fingerprints of Two-Dimensional -Phosphorus Carbide with Antisite Defects. *J. Phys. Chem. Lett.* **2023**, *14*, 214−220.
(64) Towns, J.; Cockerill, T.; Dahan, M.; Foster, I.; Gaither, K.; Grimshaw, A.; Hazlewood, V.; Lathrop, S.; Lifka, D.; Peterson, G. D.; et al. XSEDE: Accelerating Scientific Discovery. *Comput. Sci. Eng.* **2014**, *16*, 62−74.

https://doi.org/10.1021/acs.jpcc.3c06267
J. Phys. Chem. C 2023, 127, 21930−21939